JPET Fast Forward. Published on January 15, 2020 as DOI: 10.1124/jpet.119.262469
This article has not been copyedited and formatted. The final version may differ from this version.

Title Page

Arsenite-induced mitochondrial superoxide formation: time and concentration requirements for the effects of the metalloid on the endoplasmic reticulum and mitochondria

Andrea Guidarelli, Liana Cerioni, Mara Fiorani, Alessia Catalani and Orazio Cantoni

Department of Biomolecular Sciences, University of Urbino Carlo Bo, via Saffi 2, 61029 Urbino (PU), Italy.

JPET Fast Forward. Published on January 15, 2020 as DOI: 10.1124/jpet.119.262469
This article has not been copyedited and formatted. The final version may differ from this version.

Running Title: Arsenite requirements for mitochondrial superoxide formation

Corresponding author: Orazio Cantoni, Dipartimento di Scienze Biomolecolari, Sezione di Farmacologia e Igiene, Università degli Studi di Urbino, Via S. Chiara 27, 61029 Urbino (PU), Italy. Tel: +39-0722-303523; Fax: +39-0722-305470; e-mail: orazio.cantoni@uniurb.it

Number of text pages: 36

Number of tables: 0

Number of figures: 5

Number of references: 40

Number of Words

Abstract: 242

Introduction: 730

Discussion: 1603

Abbreviations:

2-APB, 2-aminoethoxydiphenyl borate; AA, L-ascorbic acid; Cf, caffeine; $[Ca^{2+}]_c$, cytosolic Ca^{2+} concentration; $[Ca^{2+}]_m$, mitochondrial Ca^{2+} concentration; DHR, dihydrorhodamine 123; DPI, diphenyleneiodonium; ER, endoplasmic reticulum; IP_3R, inositol-1,4,5-trisphosphate receptor; MCU, mitochondrial calcium uniport; $MitoO_2^{-\cdot}$, mitochondrial $O_2^{-\cdot}$; MPT, mitochondrial permeability transition; $O_2^{-\cdot}$, superoxide; PBS, phosphate-buffered saline; ROS, reactive oxygen species; RD-cells; respiration-proficient cells; RP-cells, respiration-proficient cells; Ry, ryanodine; SVCT, sodium-AA co-transporter; Trx2, thioredoxin-2.

Recommended section assignment: Toxicology

JPET Fast Forward. Published on January 15, 2020 as DOI: 10.1124/jpet.119.262469
This article has not been copyedited and formatted. The final version may differ from this version.

ABSTRACT

The present study used human myeloid leukemia U937 cells, a versatile promonocytic cellular system which, based on its endoplasmic reticulum (ER)/mitochondria functional relationships, respond to low micromolar concentrations of arsenite with a single, defined mechanism of superoxide ($O_2^{-\cdot}$) formation. Under these conditions, we observe an initial Ca^{2+} mobilization from the ER associated with the mitochondrial accumulation of the cation, followed by Ca^{2+}-dependent mitochondrial $O_2^{-\cdot}$ ($mitoO_2^{-\cdot}$) formation. These events, barely detectable after 3 h were better appreciated at 6 h. We found that remarkably shorter exposure to, and lower concentrations of, arsenite are required to induce extensive O_2^{-} formation in cells supplemented with inositol-1,4,5-trisphosphate receptor (IP_3R) or ryanodine receptor (RyR) agonists. Indeed, nanomolar arsenite induced maximal $O_2^{-\cdot}$ formation after only 10 min of exposure, and this response was uniquely dependent on the enforced mitochondrial Ca^{2+} accumulation. The dramatic anticipation of, sensitization to, the effects of arsenite caused by the IP_3R or RyR agonists was accompanied by a parallel significant genotoxic response in the absence of detectable mitochondrial dysfunction and cytotoxicity. We conclude that the prolonged, low micromolar arsenite exposure paradigm resulting in $mitoO_2^{-\cdot}$ formation is necessary to affect Ca^{2+} homeostasis and accumulate the cation in mitochondria. The arsenite requirements to promote $mitoO_2^{-\cdot}$ formation in the presence of sufficient mitochondrial Ca^{2+} were instead remarkably lower in terms of both concentration and time of exposure. These conditions were associated with the induction of extensive DNA strand scission in the absence of detectable signs of toxicity.

Significance Statement

In RP-cells, arsenite causes mitochondrial Ca^{2+} accumulation ($[Ca^{2+}]_m$) and Ca^{2+}-dependent mitochondrial superoxide formation. We now report that the second event requires remarkably lower concentrations of /time of exposure to the metalloid than the former. Indeed, a brief exposure to nanomolar levels of arsenite produced maximal effects under conditions in which the $[Ca^{2+}]_m$ was increased by IP_3R or RyR agonists. Hence, specific substances or conditions enhancing the $[Ca^{2+}]_m$,

JPET Fast Forward. Published on January 15, 2020 as DOI: 10.1124/jpet.119.262469
This article has not been copyedited and formatted. The final version may differ from this version.

may potentiate the deleterious effects of arsenite by selectively increasing mitochondrial superoxide formation.

Introduction

Arsenite is a well-established human carcinogen (International Agency for Research on Cancer (IARC, 2004) which, due to its ubiquitous presence in the environment, represents a serious threat for millions of people (Shakoor et al., 2017). Ingestion of contaminated drinking water by populations from various parts of the planet has been indeed associated to the induction of different types of tumours (lung, skin, liver, bladder and kidney (Sankpal et al., 2012; Shakoor et al., 2017; Zhou and Xi, 2018)), as well as other non-malignant diseases affecting various tissues and organs (Flora, 2011; Shakoor et al., 2017).

Arsenite therefore mediates a wide spectrum of deleterious effects, bearing numerous consequences in different cells and organs, a complex scenario in apparent contrast with the simple mechanism often implicated in the effects of the metalloid. More specifically, the opinion of various groups is that a large proportion of the critical effects mediated by arsenite results from the intermediate formation of reactive oxygen species (ROS) (Flora, 2011; Minatel et al., 2018)

Hence, the impact of the metalloid in different cell types should depend on their susceptibility to arsenite-induced ROS formation, in turn affected by an array of variables associated with the specific characteristics of the cells, tissues and organs. Different cells respond to arsenite by producing ROS *via* different mechanisms, e.g., in the mitochondrial respiratory chain (Liu et al., 2005; Guidarelli et al., 2015; Guidarelli et al., 2016a), *via* NADPH oxidase activation (Smith et al., 2001; Chou et al., 2004; Straub et al., 2008) or through both mechanisms (Li et al., 2014).

Mechanistic studies on arsenite cyto- geno-toxicity should therefore ideally involve the use of specific cell types, characterised by a well-defined antioxidant system, and responding to arsenite through established mechanisms of ROS formation. In this direction, we performed our initial studies on arsenite toxicity in U937 cells, from now on referred to as respiration-proficient (RP)-cells, with the demonstration that these cells uniquely produce mitochondrial superoxide ($mitoO_2^{-\cdot}$) in response to a low concentration of arsenite (Guidarelli et al., 2015; Guidarelli et al., 2016a). This ROS response

was sensitive to inhibitors of electron transport in the respiratory chain as well as to the respiration-deficient phenotype, i.e., respiration-deficient cells (RD-cells) derived from the same RP-cell line, failed to produce mito$O_2^{-\cdot}$ in response to arsenite. We then investigated the mechanism whereby arsenite mobilizes Ca^{2+} from the endoplasmic reticulum (ER) and found that the metalloid promotes an initial slow mobilization of a limited amount of the cation from the inositol-1,4,5-trisphosphate receptor (IP_3R). This response was ROS independent and mediated by the direct interaction of arsenite with this Ca^{2+} pool (Guidarelli et al., 2018). The initial IP_3R stimulation was associated with additional direct effects of the metalloid on the intraluminal crosstalk between the IP_3R and the ryanodine receptor (RyR), thereby leading to the release of large amounts of Ca^{2+} from the RyR (Guidarelli et al., 2018). This second response was therefore sensitive to RyR inhibitors and RyR down-regulation (Guidarelli et al., 2009).

Finally, the fraction of Ca^{2+} derived from the RyR was taken up by the mitochondria through the mitochondrial Ca^{2+} uniporter (MCU), in which the cation critically contributed to events promoting mito$O_2^{-\cdot}$ formation (Guidarelli et al., 2019a). That is, mito$O_2^{-\cdot}$ formation induced by arsenite in RP-cells, besides being sensitive to inhibitors of electron transport and to the respiration-deficient phenotype, was also suppressed by IP_3R, RyR and MCU inhibitors. In addition, the metalloid failed to promote mito$O_2^{-\cdot}$ formation in cells with downregulated RyR (Guidarelli et al., 2019a).

The mechanism(s) mediating ROS formation in RP-cells exposed to arsenite therefore involve(s) upstream events directly induced by the metalloid through its binding in specific sites of the ER, leading to Ca^{2+} mobilization and mitochondrial accumulation (Guidarelli et al., 2019a). The slow effects on the ER are possibly dependent on the time necessary to allow a significant cellular uptake of the metalloid and to promote effects resulting in Ca^{2+} mobilization and mitochondrial accumulation. It is however unclear whether the same prolonged exposure to specific arsenite

JPET Fast Forward. Published on January 15, 2020 as DOI: 10.1124/jpet.119.262469
This article has not been copyedited and formatted. The final version may differ from this version.

concentrations is also necessary to trigger the Ca^{2+}-dependent mitochondrial events associated with $O_2^{-\cdot}$ formation.

These considerations stimulated the present study in which we investigated the requirements for arsenite in the overall process leading to mitochondrial $O_2^{-\cdot}$ formation. More specifically, we asked the question of whether IP_3R or RyR agonist-induced enforced mitochondrial Ca^{2+} accumulation shortens the time required by, and/or lowers the concentration of, arsenite to promote the formation of mito$O_2^{-\cdot}$.

Materials and methods

Chemicals

Sodium arsenite, 2-aminoethoxydiphenyl borate (2-APB), Ry, L-ascorbic acid (AA), rotenone (Rot), caffeine (Cf), ATP, PMA, apocynin, diphenyleneiodonium (DPI), Hoechst 33342, as well most of reagent-grade chemicals were purchased from Sigma-Aldrich (Milan, Italy). Ru360 was from Thermo Fisher Scientific (Milan, Italy). Fluo-4- acetoxymethyl ester (AM), Rhod 2-acetoxymethyl ester (AM), Dihydrorhodamine 123 (DHR) and MitoSOX Red were purchased Thermo Fisher Scientific.

Antibodies

The antibodies against $p47^{phox}$ phosphorylated and $p47^{phox}$ were from Sigma-Aldrich. The antibody against thioredoxin-2 (Trx2; sc-133201) and the horseradish peroxidase-conjugated secondary antibody were from Santa Cruz (Santa Cruz, CA).

Cell culture and treatment conditions

U937 human myeloid leukemia cells, herein defined as RP-cells, were cultured in suspension in RPMI 1640 medium (Sigma-Aldrich). Culture media were supplemented with 10% fetal bovine serum (Euroclone, Celbio Biotecnologie, Milan, Italy), penicillin (100 units/ml), and streptomycin (100 mg/ml) (Euroclone). Cells were grown at 37° C in T-75 tissue culture flasks (Corning Inc., Corning, NY) gassed with an atmosphere of 95% air-5% CO_2. The respiration deficient phenotype (RD cells) was induced as indicated in (Guidarelli et al., 2016b).

Sodium arsenite was prepared as a 1 mM stock solution in saline A (8.182 g/l NaCl, 0.372 g/l KCl, 0.336 g/l $NaHCO_3$, and 0.9 g/l glucose, pH 7.4) and stored at 4° C. Cells (1 x 10^5 cells/ml) were exposed to arsenite, and/or other addictions, in complete RPMI 1640 culture medium, as detailed in the text, as well as in the legends to the figures. Treatments with AA were performed as detailed elsewhere (Guidarelli et al., 2014).

DHR and MitoSOX red fluorescence assay

The cells were supplemented with either 10 μM DHR or 5 μM MitoSOX Red 30 min and subsequently exposed for the last 10 min to arsenite. In other experiments, cells were exposed for increasing time intervals to arsenite, and DHR was added to the culture medium in the last 30 min of incubation. After the treatments, the cells were washed three times with saline A and fluorescence images were captured with a BX-51 microscope (Olympus, Milan, Italy), equipped with a SPOT-RT camera unit (Diagnostic Instruments, Delta Sistemi, Rome, Italy) using an Olympus LCAch 40 x/0.55 objective lens. The excitation and emission wavelengths were 488 and 515 nm (DHR) and 510 and 580 nm (MitoSOX red), with a 5-nm slit width for both emission and excitation. Images were collected with exposure times of 100-400 ms, digitally acquired and processed for fluorescence determination at the single cell level on a personal computer using ImageJ software. Mean fluorescence values were determined by averaging the fluorescence values of at least 50 cells/treatment condition/experiment.

Measurement of intracellular free calcium levels and mitochondrial Ca^{2+}

Cells were treated for 30 min with either 4 μM Fluo-4-acetoxymethyl ester or 10 μM Rhod 2-acetoxymethyl ester and subsequently exposed for the last 10 min to arsenite. After the treatments, the cells were washed three times with saline A and subsequently analysed with a fluorescence microscope. The resulting images were taken and processed as described above. The excitation and emission wavelengths were 488 and 515 nm (Fluo-4), and 540 and 590 nm (Rhod-2) with a 5-nm slit width for both emission and excitation. Images were collected with exposure times of 100-400 ms, digitally acquired and processed for fluorescence determination at the single cell level on a personal computer using the J-Image software. Mean fluorescence values were determined by averaging the fluorescence values of at least 50 cells/treatment condition/experiment.

Western blot analysis

After treatments, the cells were lysed as described in Guidarelli et al.(Guidarelli et al., 2019a). Equal amounts of proteins (25 µg) were loaded in each lane, separated by polyacrylamide gel electrophoresis in the presence of sodium dodecyl sulfate, transferred to polyvinyldiene difluoride membranes and probed with antibodies against phosphorylated $p47^{phox}$ or $p47^{phox}$. Details on Western blotting apparatus and conditions are reported elsewhere (Guidarelli et al., 2019a). Antibody against $p47^{phox}$ was used to assess the equal loading of the lanes.

Redox Western blot analysis

The Trx2 redox state was estimated by redox Western blots as described in (Folda et al., 2016). .Briefly, after treatments, the cells (2.5×10^6) were washed with phosphate buffer saline (136 mM NaCl, 10 mM Na_2HPO_4, 1.5 mM KH_2PO_4, 3 mM KCl; pH 7.4) and re-suspended in 150 µl urea lysis buffer (100 mM Tris/HCl, pH 8.2; urea 8 M; ethylenediaminetetraacetic acid 1 mM) containing 10 mM iodoacetoamide. The samples were then incubated for 20 min at 37 °C and centrifuged at 14000 x g for 1 min. 10 volumes of cold acetone/1M HCl (98:2) were added to the supernatants and the pellets were washed twice with acetone/1M HCl/H_2O (98:2:10). The pellets were re-suspended in 60 µl of urea lysis buffer containing 3.5 mM dithiothreitol and, after a 30 min incubation at 37 °C, supplemented with 30 mM iodoacetoamide and incubated for a further 30 min at 37° C. Samples were then subjected to urea- polyacrylamide gel electrophoresis (7 M urea and 7% acrylamide) under non-reducing conditions and blotted (Folda et al., 2016).

Fluorogenic caspase 3 assay

Caspase 3-like activity was monitored as described in Fiorani *et al.* (Fiorani et al., 2018). Briefly, the cells were lysed and aliquots of the extract (30 µg proteins) were incubated with 12 µM of Ac-DEVD-AMC, at 30°C. Caspase 3-like activity was determined fluorometrically (excitation at 360 nm and emission at 460 nm) by quantifying the release of aminomethylcoumarin (AMC) from cleaved caspase 3 substrate (Ac-DEVD-AMC) at appropriate intervals.

Analysis of apoptosis with Hoechst 33342 assay

After treatments, the cells were incubated for 5 min in the presence of 10 μM Hoechst 33342 and then analysed with a fluorescence microscope to assess their nuclear morphology (chromatin condensation and fragmentation). Cells with homogeneously stained nuclei were considered viable.

Cytotoxicity assay

After treatments with arsenite, the number of viable cells was estimated with the trypan blue exclusion assay. Briefly, an aliquot of the cell suspension was diluted 1:2 (v/v) with 0.4% trypan blue and the viable cells (*i.e.*, those excluding trypan blue) were counted with a hemocytometer.

Alkaline-halo assay

DNA single-strand breakage was determined using the alkaline halo assay developed in our laboratory (Crimella et al., 2011). It is important to note that, although we refer to DNA strand scission throughout the text, the DNA nicks measured by this technique under alkaline conditions may in fact include alkali labile sites in addition to direct strand breaks. Details on the alkaline-halo assay and processing of fluorescence images and on the calculation of the experimental results are also given in ref. (Crimella et al., 2011). DNA single-strand breakage was quantified by calculating the nuclear spreading factor value, representing the ratio between the area of the halo (obtained by subtracting the area of the nucleus from the total area, nucleus + halo) and that of the nucleus, from 50 to 75 randomly selected cells/experiment/treatment condition.

ATP determination

Ice-cold 5% perchloric acid was added to the cells (2 x 10^6 cells). After a 10 min incubation in an ice bath, the samples were centrifuged for 5 min at 10,000 g. The supernatants were neutralized with 3 M K_2CO_3, and the precipitates removed by centrifugation. 10% (v/v) 1 M KH_2PO_4 (pH 6.5) was added to the nucleotide-containing supernatants. The samples were then filtered through 0.22 μm pore micro-filters. The clear filtered solutions were directly analysed by

HPLC with the UV detection wavelength set at 254 nm (Stocchi et al., 1985). The liquid chromatographic system used consisted of a system gold programmable solvent module 125 and a system gold programmable solvent detector 166 (Beckman, Fullerton, CA, USA). The HPLC separation was performed–using a 15 cm x 4.6 mm, 5 µm Supelco Discovery® C18 column equipped with a 5 µm Supelguard Discovery® 18 (2 cm x 4.0 mm) (Supelco, Bellefonte, PA, USA). The mobile phase used for the separation consisted of buffer A (0.1 M KH_2PO_4) and buffer B (90:10 buffer A/methanol). The following gradient of buffer B was used: 25% in 9 min, 90% in 6 min and 100% in 2.5 min. 100% Buffer B was held for 2 min and 100–0% was reached in 6 min. Re-equilibration with buffer A for 5 min was performed before each injection.
The injected volume was 20 µl and flow rate was 1.3 ml/min.

Measurement of GSH content by high performance liquid chromatography

The cells (1 x 10^6) were suspended in 100 µl of lysis buffer, vortexed and kept for 10 min on an ice bath. Thereafter, 15 µl of 0.1 N HCl and 140 µl of precipitating solution (0.2 M-glacial meta-phosphoric acid, 5 mM sodium EDTA, 5 M NaCl) were added to the samples. After centrifugation, the supernatants were collected and kept at –20° C until the HPLC analyses. Just before analysis, 60 μl of the acid extract were supplemented with 15 μl of 0.3 M Na_2HPO_4 and 15 μl of a solution containing 20 mg of DTNB in 100 ml of sodium citrate (1% w/v). The mixture was stirred for 1 min at room temperature and, after 5 min, filtered through 0.22 µm pore micro-filters. The clear filtered solution was directly analysed by HPLC with the UV detection wavelength set at 330 nm for their GSH content (Brundu et al., 2016), using a 15 cm x 4.6 mm, 5 µm Supelco Discovery® C18 column (Supelco, Bellefonte, PA). The UV absorption was detected at 330 nm. The injection volume was 20 µl. The retention time of GSH was approximately 15.7 min.

The liquid chromatographic system used is the same described in the previous paragraph (ATP determination). The HPLC separation was performed-using a 15 cm x 4.6 mm, 5 µm Supelco Discovery®

C18 column equipped with a 5 µm Supelguard Discovery® 18 (2 cm x 4.0 mm). The mobile phase used for the separation consisted of buffer A (0.1 M KH_2PO_4) and buffer B (40:60 buffer A/acetonitrile). The following gradient of buffer B was used: 0–100% in 15 min; 100% buffer B was held for 5 min and 100–0% was reached in 20 min. Re-equilibration with buffer A for 10 min was performed before each injection. The injected volume was 20 µl and flow rate was 1 ml/min.

Statistical analysis

The results are expressed as means ± SD. Statistical differences were analyzed by one-way ANOVA followed by Dunnett's test for multiple comparison or two-way ANOVA followed by Bonferroni's test for multiple comparison using Prism 6.0 software (GraphPad Software). A value of $p < 0.05$ was considered significant.

Results

RyR or IP_3R agonists burst ROS formation after a very short time of exposure to very low concentrations of arsenite

In keeping with our recent findings (Fiorani et al., 2018), exposure of RP-cells to 2.5 μM arsenite leads to a very slow, time-dependent DHR-fluorescence response, barely detectable after 3 h, more clearly appreciable at 6 h and even more significant at 16 h (Fig. 1A). It was then interesting to observe that this time-dependence is lost under conditions in which the cells also receive IP_3R or RyR agonists in the last 10 min of arsenite exposure. More specifically, we found that 100 μM ATP (an agonist of metabotropic purinergic receptors causing IP_3R activation (Berridge, 1993), or 10 mM Cf (a RyR agonist) (Meissner, 2017), causes a remarkable leftward shift in the time-dependence of the DHR-fluorescence response mediated by the metalloid. Indeed, the responses detected in cells exposed to arsenite alone for 16 h were identical to those observed 1 or 2 h after addition of the metalloid under conditions of ATP or Cf supplementation in the final 10 min. In order to determine the effects mediated by shorter exposure to arsenite, we changed the above experimental protocol and loaded the cells with DHR prior to arsenite exposure. Interestingly, the fluorescence responses detected after a 30 min treatment with arsenite, with ATP or Cf added in the last 10 min, or even under conditions of concomitant 10 min exposure to the metalloid and ATP, or Cf, (Fig.1B) were identical to those described above and illustrated in Fig. 1A. The concentrations of ATP and Cf were selected on the bases of previous concentration-dependence studies showing that, under these conditions, both agents produce maximal increases in the cytosolic ($[Ca^{2+}]_c$) and mitochondrial ($[Ca^{2+}]_m$) Ca^{2+} concentrations (Guidarelli et al., 2018). The enhancing effects of ATP and Cf on the arsenite-induce DHR-fluorescence response displayed the same concentration-dependence (not shown).

The next question addressed was on the arsenite concentration dependence. For this purpose, the cells were treated for 10 min with increasing concentrations of arsenite associated with either ATP

or Cf. The results obtained in these experiments are shown in Fig. 1C, and indicate that ROS formation is not further increased at arsenite concentrations greater than 2.5 μM which, on the bases of the above results, was somewhat expected. These results indeed demonstrated identical $ROS^{\cdot}$ emission after very short or long term incubation with arsenite, which presumably should be associated with significantly different cellular accumulation of the metalloid. Much less expected was instead the outcome of experiments using arsenite concentrations in the sub-micromolar range. We found that the same maximal response detected with 2.5 μM arsenite was obtained using a 5 fold lower concentration of the metalloid and that 100 nM arsenite was sufficient to induce a statistically significant effect.

In order to correctly interpret the significance of the above findings, it is important to keep in mind that the fluorescence probe employed in the ROS experiments, DHR, allows the detection of H_2O_2 and various types of ROS, including the $O_2^{-\cdot}$ and the hydroxyl radical (Gomes et al., 2005). DHR also detects reactive nitrogen species, as peroxynitrite, which however cannot be produced in the specific cell line employed (Guidarelli et al., 2016a). Our previous studies (Guidarelli et al., 2015; Guidarelli et al., 2016a; Guidarelli et al., 2017), as summarised in the Introduction section, demonstrated that the slow ROS response induced by arsenite is uniquely indicative of $mitoO_2^{-\cdot}$ formation, which then dismutates to diffusible H_2O_2 causing the oxidation of DHR in the cytosolic compartment. It is instead to be determined whether the IP_3R or RyR agonists promote an enhanced DHR fluorescence response by potentiating the same, or by recruiting different, mechanisms such as NADPH oxidase.

We therefore conclude that a very short exposure to very low concentrations of arsenite promotes maximal ROS formation in the presence of ATP or Cf. The notion that these enhancing responses do not simply appear maximal because of a limitation of the assay, was established by showing that increasing concentrations of H_2O_2 promote a linear fluorescence response up to values two-three times greater than those obtained in the above experiments (not shown).

The enhancing effects of the RyR- or IP$_3$R-agonists on ROS formation are linked to the enforced mitochondrial Ca^{2+} accumulation

We performed experiments to determine the mechanism of ROS formation induced by arsenite in cells supplemented with ATP, or Cf. In recent studies we investigated the effects of these agonists on RP-cell Ca^{2+} homeostasis (Guidarelli et al., 2018; Guidarelli et al., 2019a) and therefore decided to recapitulate some of these findings, to finally determine whether these responses are affected by arsenite. In other words, we tested the effect of the short-term co-exposure paradigms on Ca^{2+} homeostasis.

We found that arsenite alone fails to promote detectable effects in the cytosolic Ca^{2+} concentration ($[Ca^{2+}]_c$) (Supplemental Figure 1A) and mitochondrial Ca^{2+} concentration ($[Ca^{2+}]_m$) (Supplemental Figure 1B), as expected. Cf instead promoted a weak increase in the $[Ca^{2+}]_c$ (Supplemental Figure 1A) associated with a robust increase in $[Ca^{2+}]_m$ (Supplemental Figure 1B). These responses were not affected by arsenite and, under these conditions, were insensitive to the IP$_3$R antagonist 2-APB (Maruyama et al., 1997) and prevented by Ry, a RyR antagonist (Meissner, 2017). Furthermore, the mitochondrial calcium uniport (MCU) inhibitor Ru360 (Zazueta et al., 1999) selectively abolished the increase in the $[Ca^{2+}]_m$, with hardly any effect detected on the $[Ca^{2+}]_c$.

We next found that ROS formation, determined by monitoring DHR oxidation, was not induced by arsenite alone, but was readily detected after combined exposure to the metalloid and Cf. In addition, as observed for the increase in the $[Ca^{2+}]_m$, this response was sensitive to Ry and Ru360, with hardly any effect detected with 2-APB (Fig. 1D).

In other experiments, we used ATP in the place of Cf, to induce a significantly greater increase in the $[Ca^{2+}]_c$ (Supplemental Figure 1A), associated with the same increase in $[Ca^{2+}]_m$ previously detected with the RyR agonist (Supplemental Figure 1B). These effects mediated by ATP were not

affected by arsenite and, under these conditions, were prevented by 2-APB. In addition, Ry was as effective as Ru360 in preventing the increase in $[Ca^{2+}]_m$, with only minor (Ry) or no (Ru360) effects being detected on the $[Ca^{2+}]_c$. ROS formation was observed after combined exposure to ATP and arsenite, and was sensitive to the above treatments preventing mitochondrial Ca^{2+} accumulation (Fig. 1D). Finally ATP, or Cf, failed to promote ROS formation in the absence of arsenite.

Collectively, the above results indicate that the mechanism whereby the IP_3R and RyR agonists enhance ROS formation induced by a 10 min exposure to arsenite involves enforced mitochondrial Ca^{2+} accumulation. The experimental approach employed in the above experiments also provided evidence for the specificity of the effects mediated by the antagonists and inhibitors.

Short-term exposure to arsenite in combination with a RyR, or IP_3R agonist uniquely mediates $mitoO_2^{-\cdot}$ formation

We asked the question of whether the enhancing effects mediated by IP_3R or RyR agonists are associated with an increased $mitoO_2^{-\cdot}$ formation or, rather, to the recruitment of a different mechanism, as NADPH activation.

As indicated in Fig. 2A the DHR-fluorescence responses mediated by the short term exposure to arsenite in combination with either Cf or ATP are prevented by the complex I inhibitor rotenone, as well as by AA, supplemented under conditions promoting high and low concentrations of the vitamin in the mitochondria and cytosol, respectively (Fiorani et al., 2015; Cantoni et al., 2018). In addition rotenone, or AA, failed to affect the changes in the $[Ca^{2+}]_m$ elicited by Cf, or ATP, in combination with the metalloid (Fig. 2B). Most importantly, the effects mediated by rotenone were reproduced by the respiration-deficient phenotype, i.e., RD-cells failed to respond to arsenite/ATP, or arsenite/Cf, with an increased DHR oxidation (Fig. 2A), but nevertheless responded to these treatments with increases in $[Ca^{2+}]_m$ comparable with those detected in their respiration-proficient counterparts (Fig. 2B).

The mitochondrial origin of ROS produced using the above treatment paradigms was next confirmed using MitoSOX red, a fluorochrome commonly employed for the detection of $O_2^{\cdot -}$ in the mitochondria of live cells (Mukhopadhyay et al., 2007). Indeed, as indicated in Fig. 2C, the results obtained using MitoSOX red were in line with those previously discussed for experiments using DHR. The notion that MitoSOX red, unlike DHR, only detects mitochondrial ROS was previously established by showing the exclusive sensitivity of the second probe to ROS generated *via* PMA-induced NADPH oxidase activation (Guidarelli et al., 2016b). These experiments, not reported here for the sake of brevity, were run in parallel with those described above as internal controls.

We next tested the possibility that the increase in $[Ca^{2+}]_c$ mediated by the 10 min exposure paradigm was associated with an early activation of NADPH oxidase, which at least in principle may eventually mediate downstream stimulation of mitochondrial ROS formation. For this purpose, we performed experiments using ATP, which causes a greater increase in $[Ca^{2+}]_c$ than Cf (Supplemental Figure 1A). The results illustrated in Supplemental Figure 2A indicate that the PMA-induced DHR fluorescence response, unlike the one induced by a 10 min exposure to ATP/arsenite, was sensitive to the NADPH oxidase inhibitors apocynin (10 μM) and DPI (1 μM) (Brandes et al., 2014). Furthermore, PMA also promoted an apocynin-or DPI-sensitive $p47^{phox}$ phosphorylation, instead not detected in cells exposed for 10 min to ATP/arsenite (Supplemental Figure 2B).

In conclusion, the short-term exposure to arsenite in combination with a RyR or IP_3R agonist leads to the exclusive formation of $mitoO_2^{\cdot -}$, thereby implying that the ROS response induced by arsenite alone is slow for the simple reason that the Ca^{2+} response leading to increased $[Ca^{2+}]_m$ is also slow.

The short-term exposure to arsenite in combination with a RyR, or IP_3R, agonist fails to induce immediate or delayed toxicity, but nevertheless causes significant DNA strand scission

We initially tested whether the fast mechanism of mito$O_2^{\cdot-}$ formation triggered through the enforced mitochondrial Ca^{2+} accumulation causes immediate consequences on the thiol pool and energetic status of the cells. We found that a 10 min exposure to arsenite, Cf, or the two agents combined, fails to affect the levels of GSH (untreated cells: 35.06 $\pm$ 4.2 nmol/mg proteins) and ATP (untreated cells: 21.05 $\pm$ 2.2 nmol/proteins). Significant effects were instead detected using H_2O_2 as a positive control (not shown). In as much as Trx2 represents a critical controller of ROS emission in mitochondria (Stanley et al., 2011; Folda et al., 2016), we also tested the impact of the cocktail arsenite/Cf or /ATP on the redox state of this protein. The redox Western blot technique (Supplemental Figure 3) failed to provide evidence of Trx2 oxidation in cells exposed to arsenite alone, or combined with either Cf or ATP. In contrast, the thiol specific oxidant diamide induced a concentration dependent oxidation of Trx2, with bands appearing in the lower part of the gel.

In other experiments, the cells were treated for 10 min with 2.5 μM arsenite, alone or associated with ATP, or Cf, and subsequently analyzed after 0, 6 or 48 h of growth in drug-free medium. Under all these different conditions, we found no evidence for caspase 3 activation (Fig. 3A) and chromatin condensation or fragmentation (Fig. 3B). In addition, the cells receiving the different treatments proliferated with rates comparable with those of the untreated cell population (Fig. 3C). Continuous exposure for 48 to 2.5 μM arsenite, as we previously reported (Guidarelli et al., 2015; Guidarelli et al., 2016a; Guidarelli et al., 2017), instead caused caspase 3 activation (Fig. 3A), apoptotic DNA fragmentation (Fig. 3B) and a significant reduction of the counts of viable cells (Fig. 3C).

The short-term exposure paradigm was not associated with an immediate or delayed toxicity as a likely consequence of the reversibility of the upstream effects associated with ROS release. This notion was established by showing that the $[Ca^{2+}]_c$ (Fig. 3D), $[Ca^{2+}]_m$ (Fig. 3E) and the DHR fluorescence response (Fig. 3F) returned to control levels after 6 h of post-treatment incubation.

We next performed experiments in which the cells were treated with arsenite/ATP, or arsenite/Cf, and then processed for the analysis of DNA strand scission using the alkaline halo assay, a technique developed in our laboratory to detect these lesions at the single cell level with a sensitivity comparable with that of the comet assay (Guidarelli et al., 2017). Supplemental Figure 4 provides typical images from ethidium bromide stained cells previously exposed for 30 min to arsenite (B), or for 10 min to ATP (C) or Cf (D), which all appeared similar to untreated cells (A). A typical image of cells with damaged DNA, i.e. displaying evidence for an increased halo/reduced nuclear remnant, was instead obtained from cells exposed for 6 h to arsenite (panel G). Interestingly, the size of the halo increased significantly also in cells exposed for 30 min to the metalloid and ATP (E), or Cf (F), in the final 10 min of incubation.

The time-dependence of the DNA strand scission was then measured in cells exposed for increasing time intervals to arsenite, with or without a final 10 min addition of either ATP or Cf. As shown in Fig. 4A, the nuclear spreading factor slowly increased in cells exposed to the metalloid alone, with kinetics comparable with those describing the rate of ROS formation (Fig. 1A). Accumulation of DNA lesions was instead significantly faster in cells receiving the treatments with the metalloid and ATP, or Cf, with a very small delay in comparison with the kinetics of ROS formation detected under the same conditions (Fig. 1A).

We next established the arsenite concentration-dependence for the DNA strand scission observed after 30 min with the supplementation of ATP or Cf in the last 10 min of incubation. Under these conditions, the metalloid alone failed to produce significant effects (Fig. 4B). Maximal DNA strand scission was instead observed in cells exposed to $\geq$ 0.5-1 μM arsenite, with ATP or Cf.

Finally, the results illustrated in Fig. 4C indicate that the genotoxic response induced by a 30 min exposure to 1 μM arsenite, associated with ATP, or Cf, is suppressed by treatments/manipulation abolishing ROS formation at the level of the mitochondrial respiratory chain, i.e., rotenone, AA and

JPET Fast Forward. Published on January 15, 2020 as DOI: 10.1124/jpet.119.262469
This article has not been copyedited and formatted. The final version may differ from this version.

the respiration-deficient phenotype, or preventing mitochondrial Ca^{2+} accumulation, i.e., Ry and Ru360. 2-APB selectively prevented DNA strand scission in cells exposed to arsenite/ATP.

We therefore conclude that the short-term exposure to arsenite in combination with RyR or IP_3R agonists fails to produce immediate or delayed toxicity, but nevertheless causes rapid and extensive DNA strand scission entirely attributable to enforced mitochondrial Ca^{2+} accumulation and Ca^{2+}-dependent mito$O_2^{\cdot-}$ formation.

Discussion

The present study was performed with the aim of investigating the requirements for arsenite in the specific events leading to mito$O_2^{-\cdot}$ formation. For this purpose, we used a mechanism-based approach, taking advantage of a versatile cell line RP-cells, characterised by a specific spatial organization of the ER, in which arsenite uniquely mediates mito$O_2^{-\cdot}$ formation (Guidarelli et al., 2019a). Based on our recent (Guidarelli et al., 2019a; Guidarelli et al., 2019b) and current findings, this spatial organization of the ER (IP_3R *vs* RyR) and the close apposition of the RyR with the mitochondria represents a *conditio sine qua non* for the arsenite-induced mito$O_2^{-\cdot}$ formation. As a consequence, the results obtained using RP-cells are likely representative of all cell types responding to arsenite with mito$O_2^{-\cdot}$ formation.

Our previous findings (Fiorani et al., 2018) indicated that exposure of RP-cells to 2.5 μM arsenite is associated with a slow and progressive formation of mito$O_2^{-\cdot}$ mediated by at least two separate events. The first one is related to the direct effects of the metalloid on the ER, resulting in Ca^{2+} mobilization and increased $[Ca^{2+}]_c$ (Guidarelli et al., 2018). This response appears slow and requires the micromolar concentration of arsenite apparently needed to target the IP_3R, and the crosstalk between this channel and the RyR (Guidarelli et al., 2018). These responses are then associated with the mitochondrial accumulation of Ca^{2+} through the MCU, necessary -but not sufficient- for mito$O_2^{-\cdot}$ formation (Guidarelli et al., 2019a). The second event, also necessary -but not sufficient- for the Ca^{2+}-dependent mito$O_2^{-\cdot}$ formation (Guidarelli et al., 2019a), is instead mediated by arsenite in a mitochondrial target, possibly the respiratory chain, and requires still undetermined durations of exposure to, and concentrations of, the metalloid.

In the present study, we took advantage of IP_3R and RyR agonists to enforce Ca^{2+} mobilization and then investigate the arsenite requirements for this second effect on mitochondria. Using a general probe, DHR, we obtained evidence for an anticipated ROS response that appeared maximal even using the 10 min treatment with 2.5 μM arsenite combined with either ATP or Cf. Furthermore, using

the 10 min co-exposure paradigm, we obtained evidence for significant ROS formation, detectable after exposure to 100 nM arsenite, and maximal at a 0.5 μM concentration of the metalloid.

These results lead to the conclusion that short exposure times of exposure to low concentrations of the metalloid are required to maximally generate ROS under optimal conditions of Ca^{2+} availability. As a corollary, the longer times of exposure and higher concentrations of the metalloid normally employed to generate similar effects appear to be uniquely functional to Ca^{2+} mobilization from the ER.

The second part of this study addressed the mechanism whereby the 10 min exposure to arsenite and the Ca^{2+}-mobilizing agents mediates the ROS response. In the case of Cf, the cation was derived from the RyR and mitochondrial Ca^{2+} accumulation was sensitive to Ry as well as to Ru360. Interestingly ATP, although resulting in a significant increase in the $[Ca^{2+}]_c$ through IP_3R stimulation (Guidarelli et al., 2019a), nevertheless caused a mitochondrial accumulation of the cation also entirely derived from RyR. Hence, mitochondrial Ca^{2+} accumulation was also sensitive to Ry and Ru360, as in the case of Cf.

These results indicate that the effects of the IP_3R and RyR agonists are dependent on their ability to induce mitochondrial Ca^{2+} accumulation. The fact that in these cells the RyR is localised in close apposition with the mitochondria (Guidarelli et al., 2019a), favours extensive mitochondrial Ca^{2+} accumulation under conditions in which the cation is released by the RyR (Eisner et al., 2013; Fauconnier et al., 2013; Delmotte and Sieck, 2015; Raffaello et al., 2016; Hirabayashi et al., 2017).

These observations also provided the experimental ground to determine that ROS formation was mediated by the increased $[Ca^{2+}]_m$, with hardly any role detected for the increased $[Ca^{2+}]_c$. Indeed, the DHR-fluorescence response mediated by arsenite/Cf, or /ATP was sensitive to treatments preventing mitochondrial Ca^{2+} accumulation and independent on the $[Ca^{2+}]_c$. For example, ATP produced a greater increase in $[Ca^{2+}]_c$ than Cf, but their effects on ROS formation were identical.

Most importantly, Ru360 in both circumstances prevented the increase in $[Ca^{2+}]_m$ and ROS formation, but did not produce effects on the $[Ca^{2+}]_c$.

The notion that ROS formation is mediated by the increasd $[Ca^{2+}]_m$ may indicate that ROS are produced within these organelles. This notion was established by showing that the DHR-fluorescence response evoked by arsenite/Cf, or /ATP, was sensitive to rotenone, the respiration deficient phenotype, or AA. Note that RP-cells express high affinity sodium-AA co-transporter (SVCT2) (Km = 26.96 ± 1.46 μM) in their plasma and mitochondrial membranes (Fiorani et al., 2015). It follows that in these cells, exposure to suboptimal concentrations of AA, lower than/close to the Km for SVCT2 leads to the accumulation of low cytosolic and very high mitochondrial levels of the vitamin, thereby providing an excellent tool to selectively scavenge $mitoO_2^{-\cdot}$ (Cantoni et al., 2018).

The formation of $mitoO_2^{-\cdot}$ in cells exposed to arsenite/ATP or /Cf, was also demonstrated in experiments in which MitoSOX red, that only detects mitochondrial ROS (Mukhopadhyay et al., 2007), was used in the place of DHR. Using this probe we could recapitulate all the results obtained with DHR, including the inhibitory effects mediated by agents resulting in mitochondrial Ca^{2+} accumulation, as well as by treatments/conditions impairing the ability of mitochondria to generate ROS.

The above findings therefore convincingly demonstrate that $mitoO_2^{-\cdot}$ is the only species generated by arsenite/ATP /Cf, a conclusion ruling out the possible involvement of NADPH oxidase(s). However, since this system is considered of pivotal importance in arsenite toxicology (Chou et al., 2004; Straub et al., 2008; Guidarelli et al., 2016b), and since ATP promotes a large increase in $[Ca^{2+}]_c$, we considered important to nevertheless perform experiments directly addressing this possibility. In this direction, it is informative to remind that RP-cells express the cytosolic isoform ($p47^{phox}$ and $p67^{phox}$) of NADPH oxidase, which, besides being responsive to PMA-dependent stimulation, also respond to high arsenite concentrations (Guidarelli et al., 2016b; Fiorani et al., 2018; Guidarelli et al., 2019b). We found that NADPH oxidase inhibitors, while suppressing

the PMA-induced DHR fluorescence response, produced hardly any effect on the DHR-fluorescence response induced by arsenite/ATP. In addition, PMA, unlike arsenite/ATP, promoted significant $p47^{phox}$ phosphorylation, thereby ruling out the possibility of a contribution of NADPH oxidase in the overall ROS response induced by arsenite/ATP.

In the third part of this study, we determined that combined short-term exposure to arsenite and ATP, or Cf, fails to produce effects on the intracellular levels of GSH or ATP. Likewise, there was no evidence of detectable Trx2 oxidation, thereby implying that mitochondrial $O_2^{-\cdot}$ and H_2O_2 are effectively scavenged by the mitochondrial antioxidant network. Finally, we also failed to detect delayed toxic effects eventually leading to mitochondrial dysfunction and apoptosis.

The absence of the above responses/consequences is most likely attributable to the transient nature of the effects mediated by the metalloid in combination with the Ca^{2+}-mobilizing agent. Consistently, post-treatment incubation in fresh culture medium allowed complete recovery of the $[Ca^{2+}]_c$ and $[Ca^{2+}]_m$, and returned the rate of $mitoO_2^{-\cdot}$ formation to control levels.

The same requirements of a prolonged exposure to arsenite alone, in order to promote toxicity, were recently established in our laboratory (Guidarelli et al., 2015; Guidarelli et al., 2016a). Indeed, a 6 h exposure to arsenite, followed by post-treatment incubation in fresh culture medium, failed to bear deleterious consequences, as instead occurred in cells continuously exposed to the metalloid, experiencing a sustained increase in $[Ca^{2+}]_c$ and $[Ca^{2+}]_m$, as well as persistent $mitoO_2^{-\cdot}$ formation, mitochondrial dysfunction and apoptosis (Guidarelli et al., 2019a).

It therefore appears that the process of transient $mitoO_2^{-\cdot}$ formation encompassed by the low arsenite concentration under conditions of enforced mitochondrial Ca^{2+} accumulation is devoid of intrinsic cytotoxicity. Hence, it was interesting to observe that these same conditions were associated with the occurrence of an event relevant for arsenic-induced carcinogenesis. We found that the Ca^{2+} mobilizing agents caused a remarkable anticipation of the DNA-damaging response evoked by arsenite. These kinetics, while slightly slower, were nevertheless comparable with those observed in

experiments measuring ROS formation, which is clearly expected since a cause-effect relationship links these parameters. Consistently, a remarkable leftward shift was observed in the dose-response curves for arsenite-induced DNA strand scission after a very short time of exposure.

In conclusion, the results presented in this study provide solid experimental evidence that short term exposure to low concentrations of arsenite is required to promote the mitochondrial events associated with Ca^{2+}-dependent mito$O_2^{\cdot -}$ formation. This is in contrast with the more stringent requirements identified for the upstream Ca^{2+} mobilization, likely representing a critical limiting factor involved in the regulation of the arsenite-dependent ROS formation. That is, the presence of the metalloid is obviously necessary, but in fact, the concentration and time requirements are very low when Ca^{2+} is present. A scheme summarizing these findings is shown in Fig. 5.

Understanding the specific requirements of arsenite to induce its effects on Ca^{2+} homeostasis is of particular importance to determine the threshold limits of exposure to this dangerous environmental contaminant. It is indeed important to consider the possibility that the effects of arsenite are concomitant with those of other substances, e.g., pharmaceuticals, environmental contaminants, food additives as well as hormones and mediators, including those released under inflammatory conditions, which may enforce the mitochondrial accumulation of Ca^{2+} thereby fostering the effects of arsenite on mito$O_2^{\cdot -}$ formation.

The present study, while providing important details on the mechanism whereby arsenite promotes mito$O_2^{\cdot -}$ formation, raises concerns on possible effects mediated by apparently low levels of the metalloid and the concomitant activation of physiological, pathological and toxicological responses leading to enforced mitochondrial Ca^{2+} accumulation.

Authorship Contributions

Participated in research design: Guidarelli, Cerioni, Fiorani, Catalani, Cantoni.

Conducted experiments: Guidarelli, Cerioni, Fiorani, Catalani.

Performed data analysis: Guidarelli, Cerioni, Fiorani, Catalani, Cantoni.

Wrote or contributed to the writing of the manuscript: Guidarelli, Fiorani, Cantoni.

References

Berridge MJ (1993) Inositol trisphosphate and calcium signalling. *Nature* **361**:315-325.

Brandes RP, Weissmann N and Schroder K (2014) Nox family NADPH oxidases: molecular mechanisms of activation. *Free Radic Biol Med* **76**:208-226.

Brundu S, Palma L, Picceri GG, Ligi D, Orlandi C, Galluzzi L, Chiarantini L, Casabianca A, Schiavano GF, Santi M, Mannello F, Green K, Smietana M, Magnani M and Fraternale A (2016) Glutathione depletion is linked with Th2 polarization in mice with a retrovirus-induced immunodeficiency syndrome, murine AIDS: role of proglutathione molecules as immunotherapeutics. *J Virol* **90**:7118-7130.

Cantoni O, Guidarelli A and Fiorani M (2018) Mitochondrial uptake and accumulation of vitamin C: what can we learn from cell culture studies? *Antioxid Redox Signal* **29**:1502-1515.

Chou WC, Jie C, Kenedy AA, Jones RJ, Trush MA and Dang CV (2004) Role of NADPH oxidase in arsenic-induced reactive oxygen species formation and cytotoxicity in myeloid leukemia cells. *Proc Natl Acad Sci U S A* **101**:4578-4583.

Crimella C, Cantoni O, Guidarelli A, Vantaggiato C, Martinuzzi A, Fiorani M, Azzolini C, Orso G, Bresolin N and Bassi MT (2011) A novel nonsense mutation in the APTX gene associated with delayed DNA single-strand break removal fails to enhance sensitivity to different genotoxic agents. *Hum Mutat* **32**:E2118-2133.

Delmotte P and Sieck GC (2015) Interaction between endoplasmic/sarcoplasmic reticulum stress (ER/SR stress), mitochondrial signaling and Ca^{2+} regulation in airway smooth muscle (ASM). *Can J Physiol Pharmacol* **93**:97-110.

Eisner V, Csordas G and Hajnoczky G (2013) Interactions between sarco-endoplasmic reticulum and mitochondria in cardiac and skeletal muscle-pivotal roles in Ca^{2+} and reactive oxygen species signaling. *J Cell Sci* **126**:2965-2978.

Fauconnier J, Roberge S, Saint N and Lacampagne A (2013) Type 2 ryanodine receptor: a novel therapeutic target in myocardial ischemia/reperfusion. *Pharmacol Therap* **138**:323-332.

Fiorani M, Azzolini C, Cerioni L, Scotti M, Guidarelli A, Ciacci C and Cantoni O (2015) The mitochondrial transporter of ascorbic acid functions with high affinity in the presence of low millimolar concentrations of sodium and in the absence of calcium and magnesium. *Biochim Biophys Acta* **1848**:1393-1401.

Fiorani M, Guidarelli A, Capellacci V, Cerioni L, Crinelli R and Cantoni O (2018) The dual role of mitochondrial superoxide in arsenite toxicity: Signaling at the boundary between apoptotic commitment and cytoprotection. *Toxicol Appl Pharmacol* **345**:26-35.

Flora SJ (2011) Arsenic-induced oxidative stress and its reversibility. *Free Radic Biol Med* **51**:257-281.

Folda A, Citta A, Scalcon V, Cali T, Zonta F, Scutari G, Bindoli A and Rigobello MP (2016) Mitochondrial thioredoxin system as a modulator of cyclophilin D redox state. *Sci Rep* **6**:23071.

Gomes A, Fernandes E and Lima JL (2005) Fluorescence probes used for detection of reactive oxygen species. *J Biochem Biophys Methods* **65**:45-80.

Guidarelli A, Carloni S, Balduini W, Fiorani M and Cantoni O (2016a) Mitochondrial ascorbic acid prevents mitochondrial $O_2^{\cdot-}$ formation, an event critical for U937 cell apoptosis induced by arsenite through both autophagic-dependent and independent mechanisms. *Biofactors* **42**:190-200.

Guidarelli A, Cerioni L, Fiorani M, Azzolini C and Cantoni O (2014) Mitochondrial ascorbic acid is responsible for enhanced susceptibility of U937 cells to the toxic effects of peroxynitrite. *Biofactors* **40**:236-246.

Guidarelli A, Cerioni L, Fiorani M and Cantoni O (2009) Differentiation-associated loss of ryanodine receptors: a strategy adopted by monocytes/macrophages to prevent the DNA single-strand breakage induced by peroxynitrite. *J Immunol* **183**:4449-4457.

Guidarelli A, Fiorani M, Azzolini C, Cerioni L, Scotti M and Cantoni O (2015) U937 cell apoptosis induced by arsenite is prevented by low concentrations of mitochondrial ascorbic acid with hardly any effect mediated by the cytosolic fraction of the vitamin. *Biofactors* **41**:101-110.

Guidarelli A, Fiorani M and Cantoni O (2018) Low concentrations of arsenite target the intraluminal inositol 1, 4, 5-trisphosphate receptor/ryanodine receptor crosstalk to significantly elevate intracellular Ca^{2+}. *J Pharmacol Exp Ther* **367**:184-193.

Guidarelli A, Fiorani M, Carloni S, Cerioni L, Balduini W and Cantoni O (2016b) The study of the mechanism of arsenite toxicity in respiration-deficient cells reveals that NADPH oxidase-derived superoxide promotes the same downstream events mediated by mitochondrial superoxide in respiration-proficient cells. *Toxicol Appl Pharmacol* **307**:35-44.

Guidarelli A, Fiorani M, Cerioni L and Cantoni O (2019a) Calcium signals between the ryanodine receptor- and mitochondria critically regulate the effects of arsenite on mitochondrial superoxide formation and on the ensuing survival vs apoptotic signaling. *Redox Biol* **20**:285-295.

Guidarelli A, Fiorani M, Cerioni L and Cantoni O (2019b) The compartmentalised nature of the mechanisms governing superoxide formation and scavenging in cells exposed to arsenite. *Toxicol Appl Pharmacol* **384**:114766.

Guidarelli A, Fiorani M, Cerioni L, Scotti M and Cantoni O (2017) Arsenite induces DNA damage via mitochondrial ROS and induction of mitochondrial permeability transition. *Biofactors* **43**:673-684.

Hirabayashi Y, Kwon SK, Paek H, Pernice WM, Paul MA, Lee J, Erfani P, Raczkowski A, Petrey DS, Pon LA and Polleux F (2017) ER-mitochondria tethering by PDZD8 regulates Ca^{2+} dynamics in mammalian neurons. *Science* **358**:623-630.

International Agency for Research on Cancer (IARC) Working Group on the Evaluation of Carcinogenic Risks to Humans (2004) Some drinking-water disinfectants and contaminants, including arsenic., *IARC Monogr Eval Carcinog Risks Hum* **84**:1-477.

Li YN, Xi MM, Guo Y, Hai CX, Yang WL and Qin XJ (2014) NADPH oxidase-mitochondria axis-derived ROS mediate arsenite-induced HIF-1alpha stabilization by inhibiting prolyl hydroxylases activity. *Toxicol Lett* **224**:165-174.

Liu SX, Davidson MM, Tang X, Walker WF, Athar M, Ivanov V and Hei TK (2005) Mitochondrial damage mediates genotoxicity of arsenic in mammalian cells. *Cancer Res* **65**:3236-3242.

Maruyama T, Kanaji T, Nakade S, Kanno T and Mikoshiba K (1997) 2APB, 2-aminoethoxydiphenyl borate, a membrane-penetrable modulator of Ins(1,4,5)P_3-induced Ca^{2+} release. *J Biochem* **122**:498-505.

Meissner G (2017) The structural basis of ryanodine receptor ion channel function. *J Gen Physiol* **149**:1065-1089.

Minatel BC, Sage AP, Anderson C, Hubaux R, Marshall EA, Lam WL and Martinez VD (2018) Environmental arsenic exposure: From genetic susceptibility to pathogenesis. *Environ Int* **112**:183-197.

Mukhopadhyay P, Rajesh M, Hasko G, Hawkins BJ, Madesh M and Pacher P (2007) Simultaneous detection of apoptosis and mitochondrial superoxide production in live cells by flow cytometry and confocal microscopy. *Nat Protoc* **2**:2295-2301.

Raffaello A, Mammucari C, Gherardi G and Rizzuto R (2016) Calcium at the center of cell signaling: interplay between endoplasmic reticulum, mitochondria, and lysosomes. *Trends Biochem Sci* **41**:1035-1049.

Sankpal UT, Pius H, Khan M, Shukoor MI, Maliakal P, Lee CM, Abdelrahim M, Connelly SF and Basha R (2012) Environmental factors in causing human cancers: emphasis on tumorigenesis. *Tumour Biol* **33**:1265-1274.

Shakoor MB, Nawaz R, Hussain F, Raza M, Ali S, Rizwan M, Oh SE and Ahmad S (2017) Human health implications, risk assessment and remediation of As-contaminated water: A critical review. *Sci Total Environ* **601-602**:756-769.

Smith KR, Klei LR and Barchowsky A (2001) Arsenite stimulates plasma membrane NADPH oxidase in vascular endothelial cells. *Am J Physiol Lung Cell Mol Physiol* **280**:L442-449.

Stanley BA, Sivakumaran V, Shi S, McDonald I, Lloyd D, Watson WH, Aon MA and Paolocci N (2011) Thioredoxin reductase-2 is essential for keeping low levels of H_2O_2 emission from isolated heart mitochondria. *J Biol Chem* **286**:33669-33677.

Stocchi V, Cucchiarini L, Magnani M, Chiarantini L, Palma P and Crescentini G (1985) Simultaneous extraction and reverse-phase high-performance liquid chromatographic determination of adenine and pyridine nucleotides in human red blood cells. *Anal Biochem* **146**:118-124.

Straub AC, Clark KA, Ross MA, Chandra AG, Li S, Gao X, Pagano PJ, Stolz DB and Barchowsky A (2008) Arsenic-stimulated liver sinusoidal capillarization in mice requires NADPH oxidase-generated superoxide. *J Clin Invest* **118**:3980-3989.

Zazueta C, Sosa-Torres ME, Correa F and Garza-Ortiz A (1999) Inhibitory properties of ruthenium amine complexes on mitochondrial calcium uptake. *J Bioenerg Biomembr* **31**:551-557.

Zhou Q and Xi S (2018) A review on arsenic carcinogenesis: Epidemiology, metabolism, genotoxicity and epigenetic changes. *Regul Toxicol Pharmacol* **99**:78-88.

Footnotes

This work was supported by Ministero dell'Università e della Ricerca Scientifica e Tecnologica, Programmi di Ricerca Scientifica di Rilevante Interesse Nazionale, 2017, [Grant number: 2017FJSM9S] and by Dipartimento di Scienze Biomolecolare, Università degli Studi di Urbino Carlo Bo, Progetti Valorizzazione (2017-2018).

Legends to the figures

Fig. 1. Time- and concentration-dependence for the arsenite-induced ROS formation in the absence or presence of Ca^{2+} mobilizing agents

(A) RP-cells were exposed for increasing time intervals to 2.5 μM arsenite, supplemented in the last 30 and 10 min of incubation with respectively DHR and ATP (100 μM), or Cf (10 mM), and finally analysed for the resulting DHR fluorescence responses. (B) Cells were preloaded with DHR (30 min), treated for 10 or 30 min with arsenite and exposed to ATP, or Cf, in the last 10 min of incubation. (C) Cells were pre-loaded with DHR (30 min) and then exposed for 10 min to ATP, or Cf, with or w/o increasing concentrations of arsenite. (D) Cells pre-loaded with DHR (30 min), were exposed for 5 min to the vehicle, 2-APB (50 μM), Ry (20 μM) or Ru360 (10 μM) and finally treated for further 10 min with 2.5 μM arsenite, with or w/o ATP or Cf. After treatments, the cells were analysed for their DHR-fluorescence. Results represent the means ± SD calculated from at least three separate experiments. *$P < 0.05$, **$P < 0.01$, as compared to untreated cells (A-C two-way ANOVA followed by Bonferroni's test; D one-way ANOVA followed by Dunnet's test).

Fig. 2. ROS formation induced by short-term co-exposure to low concentrations of arsenite and the Ca^{2+} mobilizing agents takes place in the mitochondrial respiratory chain

(A-C) RP- and RD-cells pre-loaded for 30 min with DHR (A), Rhod-2-AM (B) or MitoSOX red (C),were exposed for 5 min to the vehicle, rotenone (0.5 μM) or AA (10 μM), and were finally treated for further 10 min with 2.5 μM arsenite, with or w/o ATP or Cf. After treatments, the cells were analysed for the resulting fluorescence responses. Results represent the means ± SD calculated from at least three separate experiments. *$P < 0.01$, as compared to untreated cells (one-way ANOVA followed by Dunnet's test).

Fig. 3. Mito$O_2^{-\cdot}$ generated by the short-term co-exposure to arsenite and ATP, or Cf, fails to induce toxicity

(A and B) RP-cells exposed for 10 min to 2.5 μM arsenite, with or w/oATP or Cf, and analysed for their caspase-3 activity (A) or for apoptosis, detected by measuring chromatin fragmentation/condensation (B), either immediately or after a 6 or 48 h in growth in fresh culture medium. In other experiments, the cells were grown for 48 h in the presence of arsenite (A and B). (C) RP-cells were treated as indicated above, and finally counted after growth in fresh culture medium for increasing time intervals. The closed circles indicate cells grown in the continuous presence of arsenite. (D-F) Cells were loaded (30 min) with Fluo 4-AM (D), Rhod-2-AM (E) or DHR (F) and then treated for 10 min as indicated in the figure. After treatments, the cells were processed to determine the respective fluorescence responses either immediately or after a 6 h post-incubation in fresh culture medium. Results represent the means ± SD calculated from at least three separate experiments. *$P < 0.05$, **$P < 0.01$, as compared to untreated cells (A, B, D-F one-way ANOVA followed by Dunnet's test; C two-way ANOVA followed by Bonferroni's test).

Fig. 4. Mito$O_2^{-\cdot}$ generated by the short-term co-exposure to arsenite and ATP or Cf, leads to DNA single-strand breakage.

(A) RP-cells exposed for increasing time intervals to 2.5 μM arsenite received a 10 min treatment with ATP, or Cf, at the end of the incubation and were subsequently analysed for DNA damage by the alkaline halo assay. (B) Cells exposed for 30 min to increasing concentrations of arsenite received ATP, or Cf, in the last 10 min and were then immediately analysed for DNA damage.

(C) Cells were exposed for 5 min to the vehicle, rotenone, AA, 2-PPB, Ry or Ru360, for a further 30 min to 2.5 uM arsenite, with or w/o ATP, or Cf, in the last 10 min of incubation, and finally analysed for DNA strand scission. In some experiments, the DNA-damaging response was measured in RD-cells co-exposed for 30 min to arsenite and ATP, or Cf. Results represent the means ± SD calculated from at least 3 separate experiments. *$P < 0.05$, **$P < 0.01$, as compared to untreated cells (A, B two-way ANOVA followed by Bonferroni's test; C one-way ANOVA followed by Dunnet's test).

JPET Fast Forward. Published on January 15, 2020 as DOI: 10.1124/jpet.119.262469
This article has not been copyedited and formatted. The final version may differ from this version.

Fig. 5. Arsenite requirements for maximal Ca^{2+}-dependent mito$O_2^{\cdot-}$/H_2O_2 formation

Prolonged (h) exposure to high concentrations of arsenite is necessary to target the IP_3R, and the crosstalk between this pool and the RyR, to promote RyR-derived Ca^{2+} accumulation in mitochondria. These events are favoured by the specific architecture of the ER, and by the close apposition between the RyR and mitochondria of RP-cells. Remarkably shorter exposure to significantly lower concentrations of the metalloid are instead required to maximally generate mito$O_2^{\cdot-}$ under optimal conditions of Ca^{2+} availability. This notion was clearly established by enforcing mitochondrial Ca^{2+} accumulation with IP_3R or RyR agonists, and the resulting mito$O_2^{\cdot-}$, and its dismutation product, H_2O_2, while failing to promote mitochondrial dysfunction and MPT-dependent apoptosis, nevertheless caused extensive DNA strand scission.

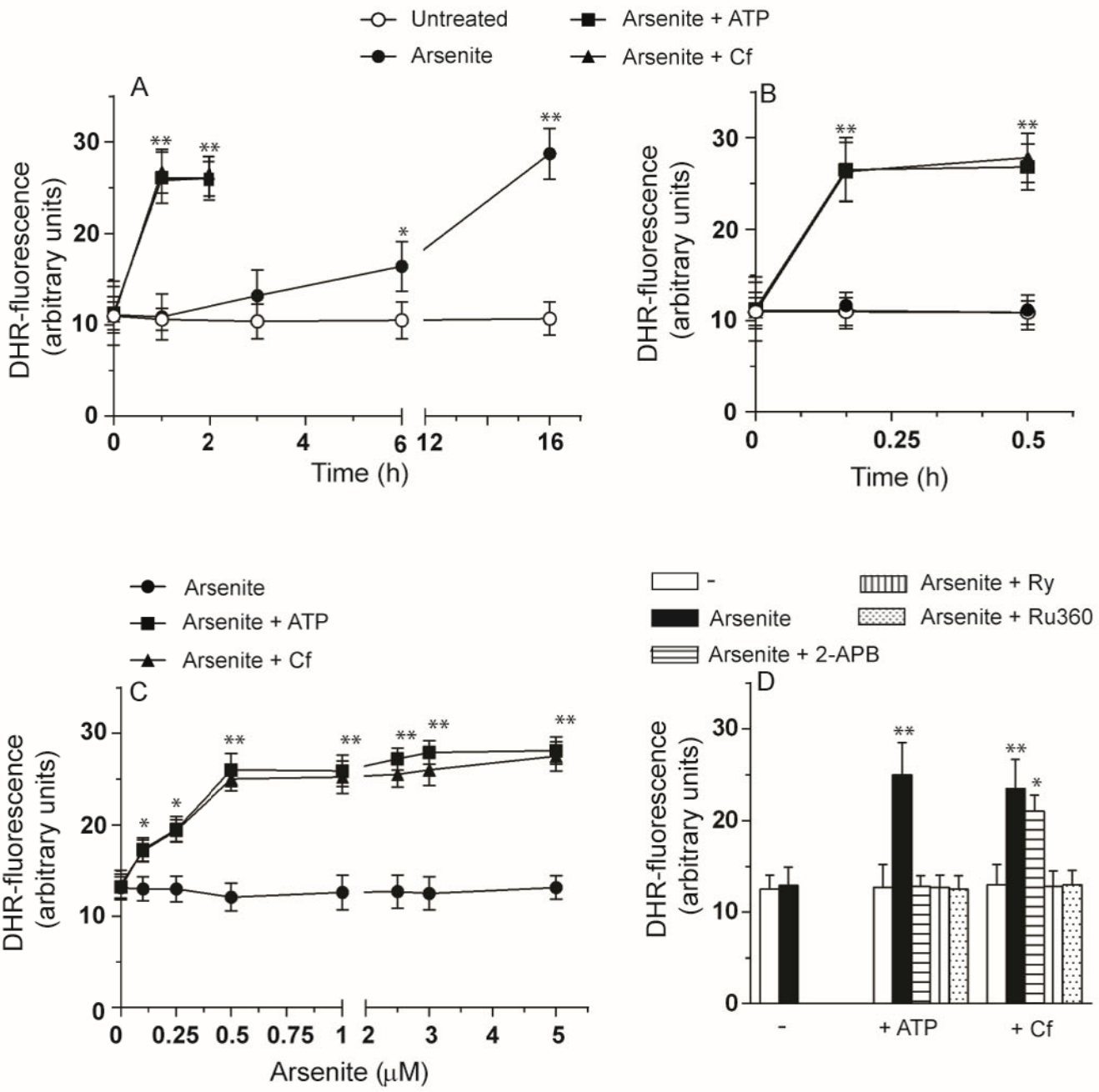

Figure 1

JPET Fast Forward. Published on January 15, 2020 as DOI: 10.1124/jpet.119.262469
This article has not been copyedited and formatted. The final version may differ from this version.

JPET Fast Forward. Published on January 15, 2020 as DOI: 10.1124/jpet.119.262469
This article has not been copyedited and formatted. The final version may differ from this version.

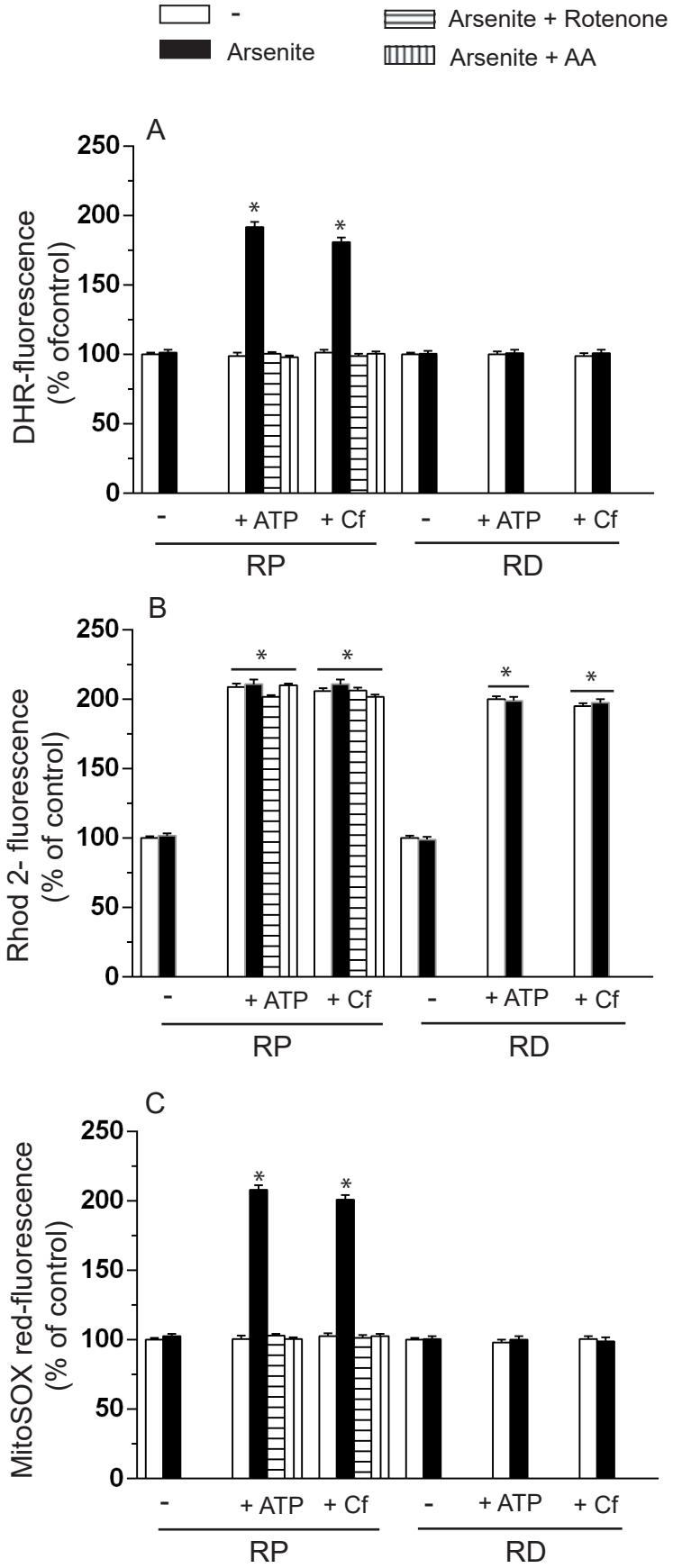

Figure 2

JPET Fast Forward. Published on January 15, 2020 as DOI: 10.1124/jpet.119.262469
This article has not been copyedited and formatted. The final version may differ from this version.

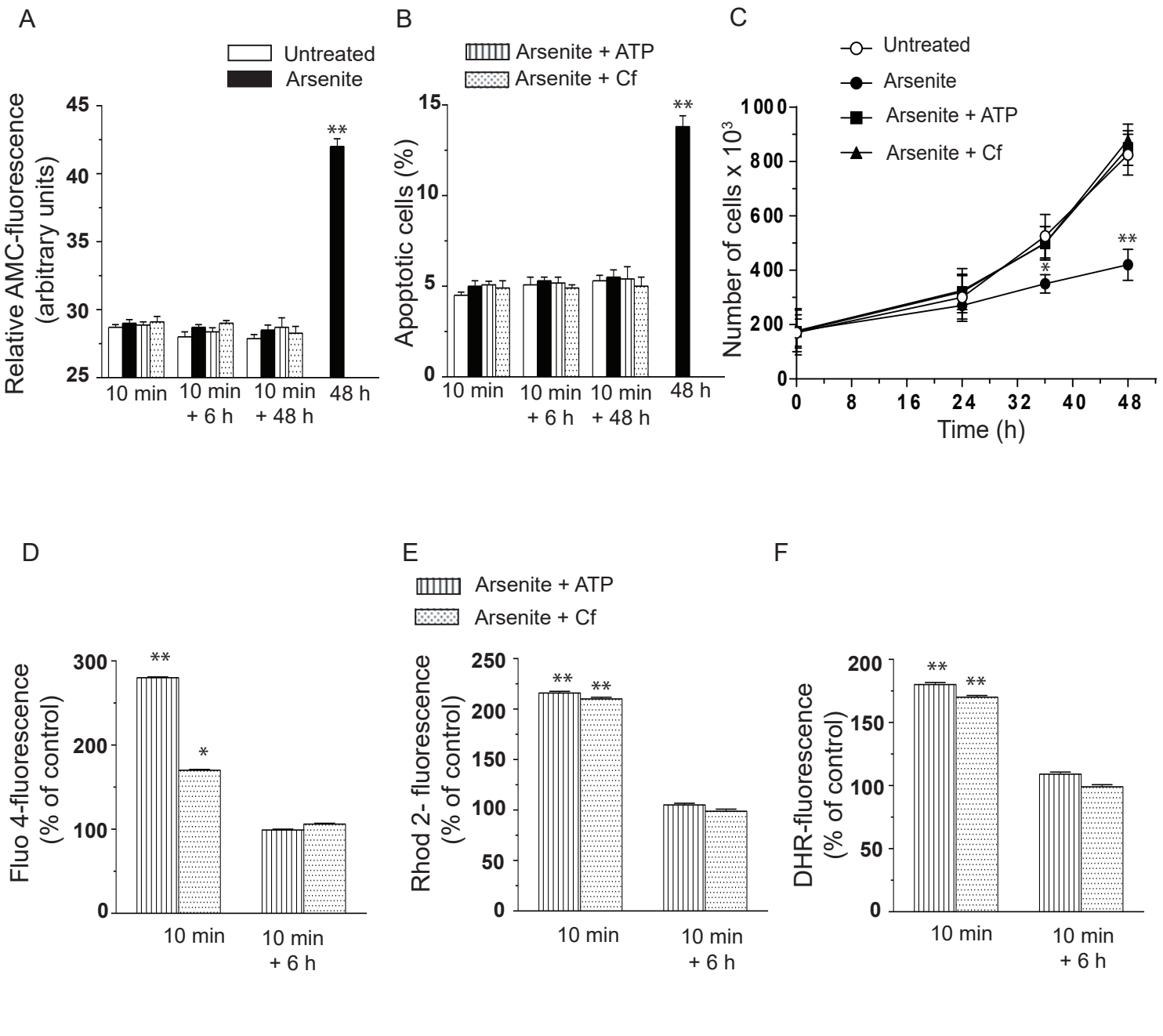

Figure 3

JPET Fast Forward. Published on January 15, 2020 as DOI: 10.1124/jpet.119.262469
This article has not been copyedited and formatted. The final version may differ from this version.

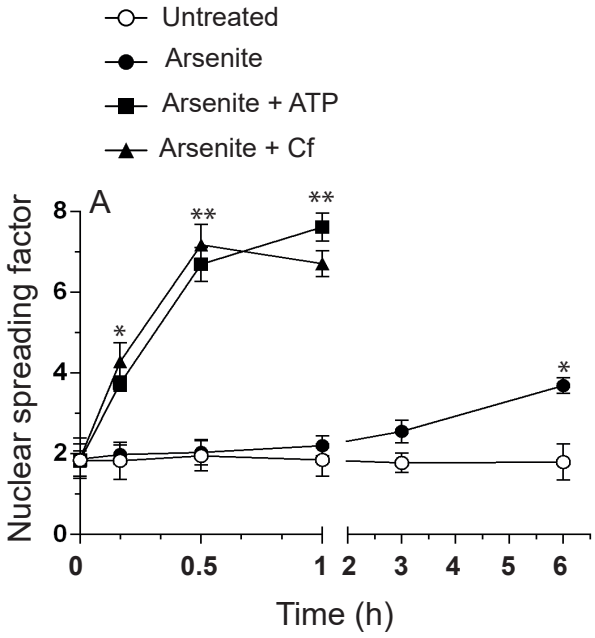

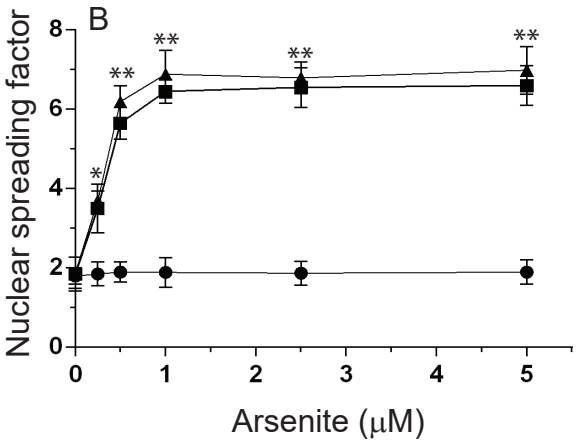

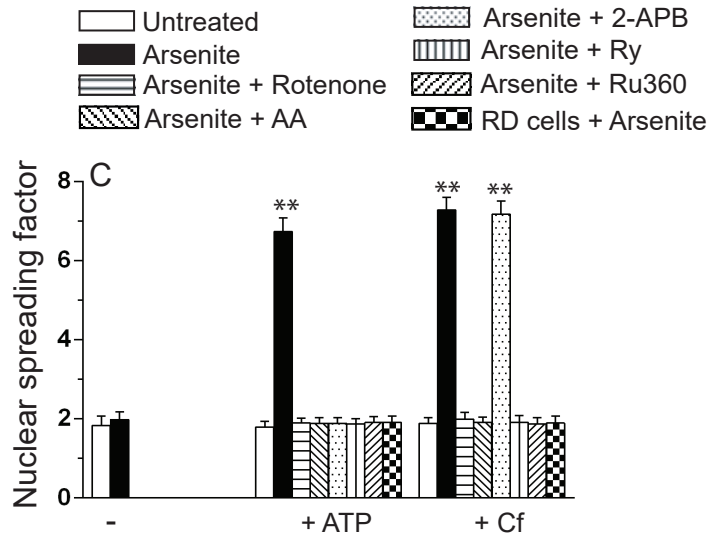

Figure 4

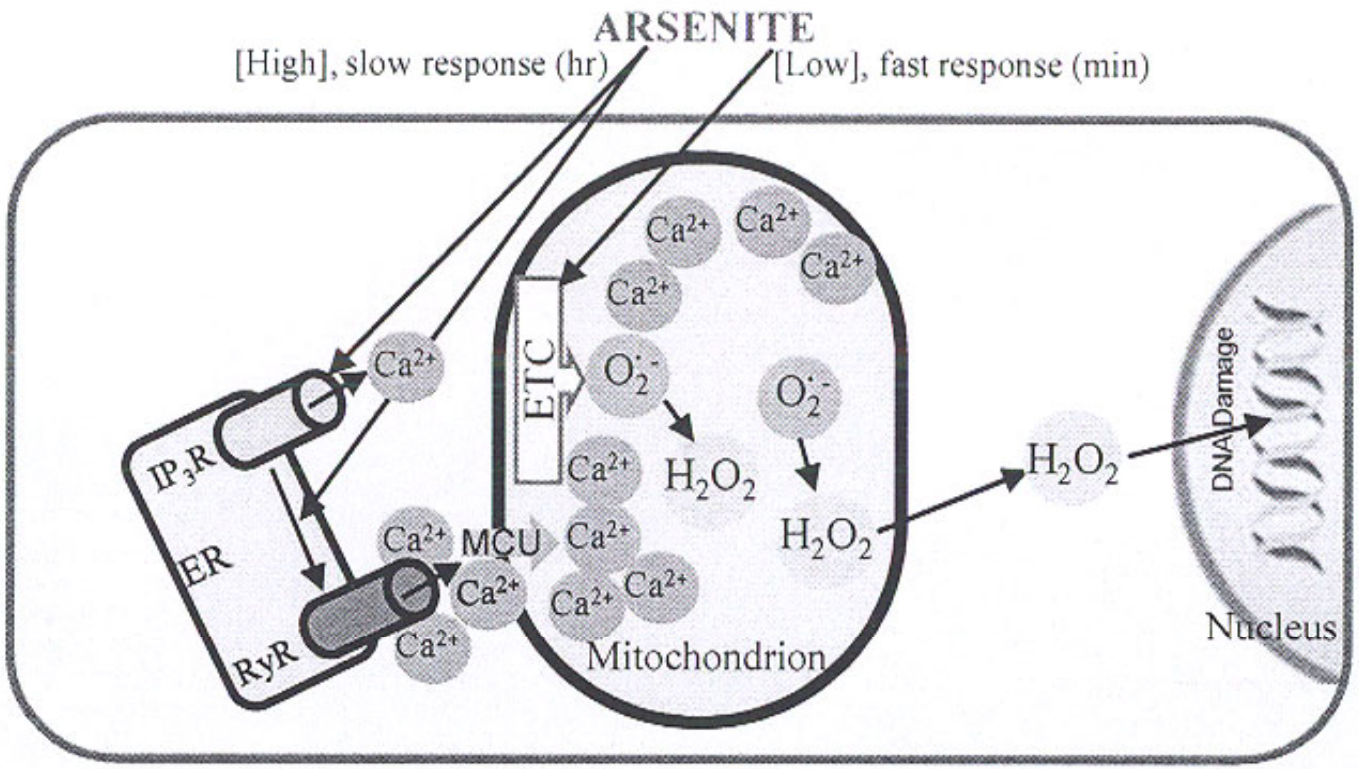

Figure 5

Arsenite-induced mitochondrial superoxide formation: time and concentration requirements for the effects of the metalloid on the endoplasmic reticulum and mitochondria

Andrea Guidarelli, Liana Cerioni, Mara Fiorani, Alessia Catalani and Orazio Cantoni
Department of Biomolecular Sciences, University of Urbino Carlo Bo, via Saffi 2, 61029 Urbino (PU), Italy.

Journal of Pharmacology and Experimental Therapeutics

Supplemental Figure 1. The effect of the short-term co-exposure to arsenite and ATP, or Cf, on Ca^{2+}-dependent homeostasis

RP-cells pre-loaded for 30 min with Fluo-4-AM (A), or Rhod-2-AM (B), were exposed for 5 min to 2-APB (50 μM), Ry (20 μM) or Ru360 (10 μM), and treated for a further 10 min with 2.5 μM arsenite, with or w/o ATP, or Cf. Cells were then analyses for their fluorescence responses. Results represent the means ± SD calculated from at least three separate experiments. *$P < 0.05$, **$P < 0.01$, as compared to untreated cells (one-way ANOVA followed by Dunnet's test).

Supplemental Figure 2. NADPH-oxidase is not involved in Ca^{2+}-dependent ROS formation induced by arsenite

(A) RP-cells pre-loaded with DHR (30 min), were exposed for 5 min to the vehicle, apocynin (10 μM) or DPI (1 μM) and for a further 10 min to the arsenite alone or associated with ATP. In some experiments, the cells were exposed for 30 min to PMA (100 ng/ml) in the absence or presence of apocynin or DPI. After treatments, the cells were analysed for DHR-fluorescence. (B) The cells treated as indicated in A were analysed for phospho p47 ^{phox} expression. The blot, representative of three separate experiments, was re-probed for p47 ^{phox}. Results represent the means ± SD calculated

from at least three separate experiments. *$P < 0.05$, **$P < 0.01$, as compared to untreated cells (H two-way ANOVA followed by Bonferroni's test; I one-way ANOVA followed by Dunnet's test).

Supplemental Figure 3. Short-term exposure to arsenite/ATP or Cf did not change the redox state of Trx2

RP-cells (2.5×10^6), treated for 10 min as detailed below, were processed for the analysis of reduced, partially oxidized and fully oxidized Trx2 thiol groups. The redox state of Trx2 was measured by urea-PAGE under non-reducing conditions. (a) control; (b) 2.5 μM arsenite; (c) arsenite and ATP (d) arsenite and Cf (e), 0.5 mM diamide (60 min), (f) 1 mM diamide (60 min), (g) control, (h) mobility standard.

Supplemental Figure 4. Short-term exposure to arsenite/ATP or Cf is associated with the induction of DNA single-strand breakage.

Representative micrographs of cells treated for 30 min with the vehicle (A), 2.5 μM arsenite (B), ATP (in the last 10 min, C), Cf (in the last 10 min, D), arsenite and ATP (E) or arsenite and Cf (F) and finally processed with the alkaline halo assay. (G) micrograph of cells exposed for 6 h to arsenite.

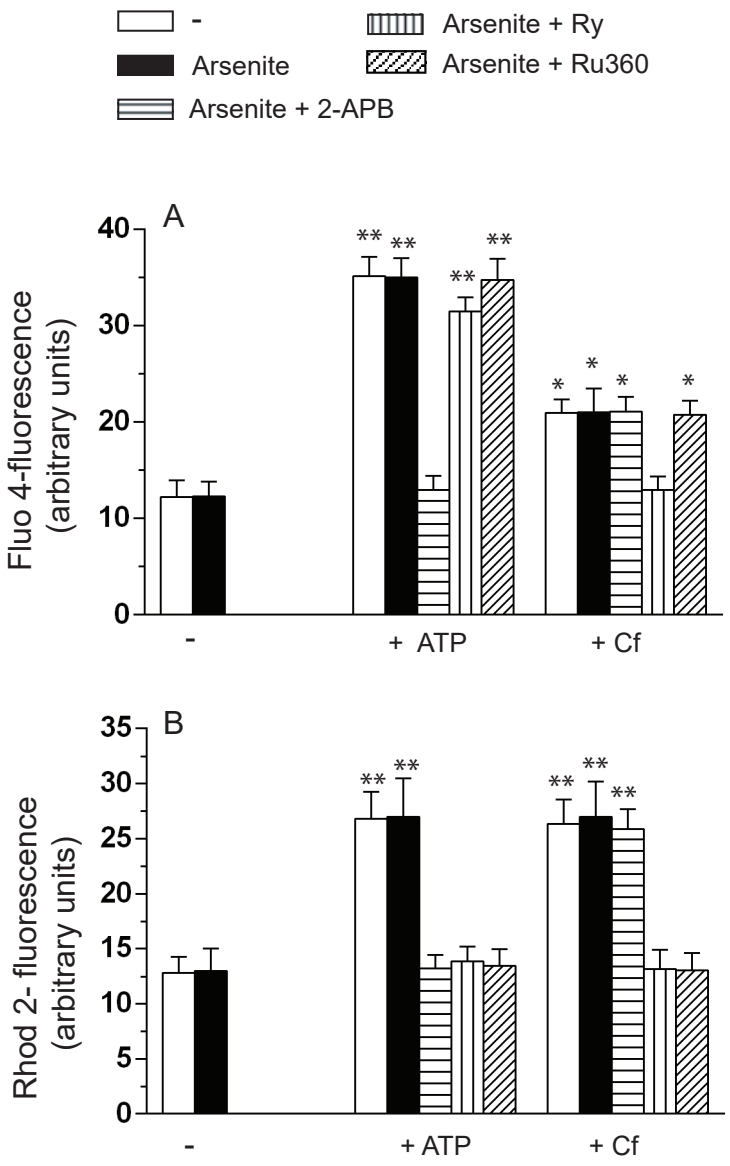

Supplemental Figure 1

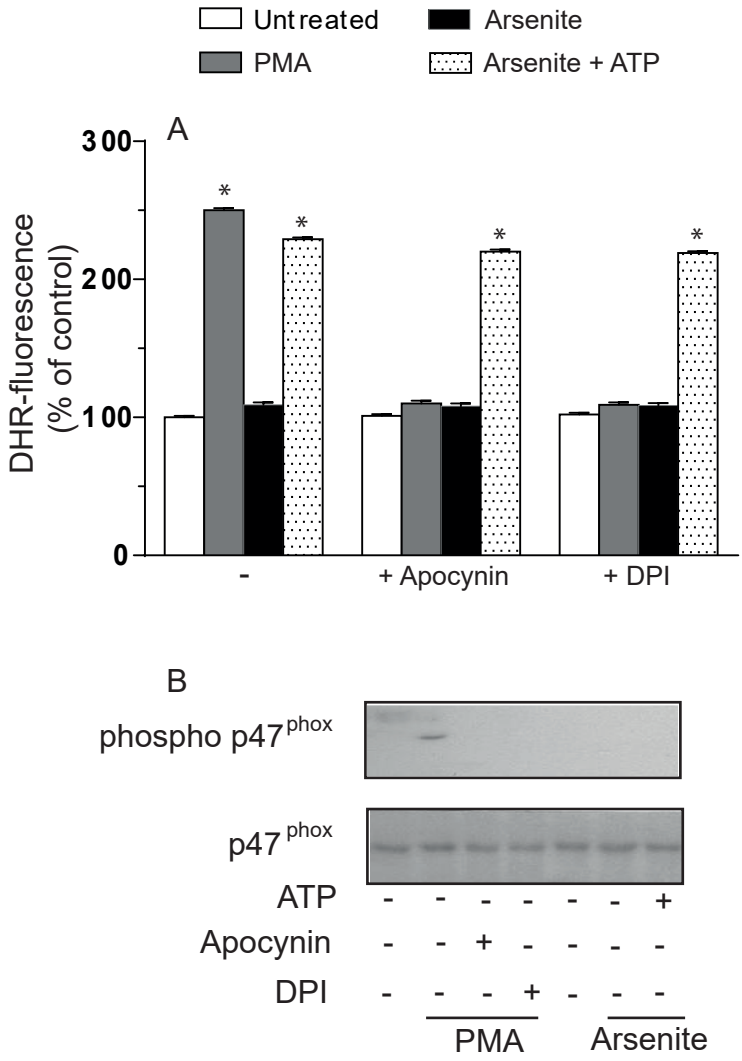

Supplemental Figure 2

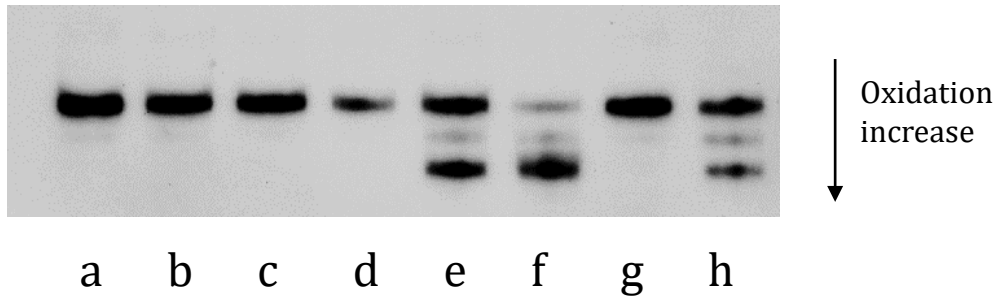

Supplemental Figure 3

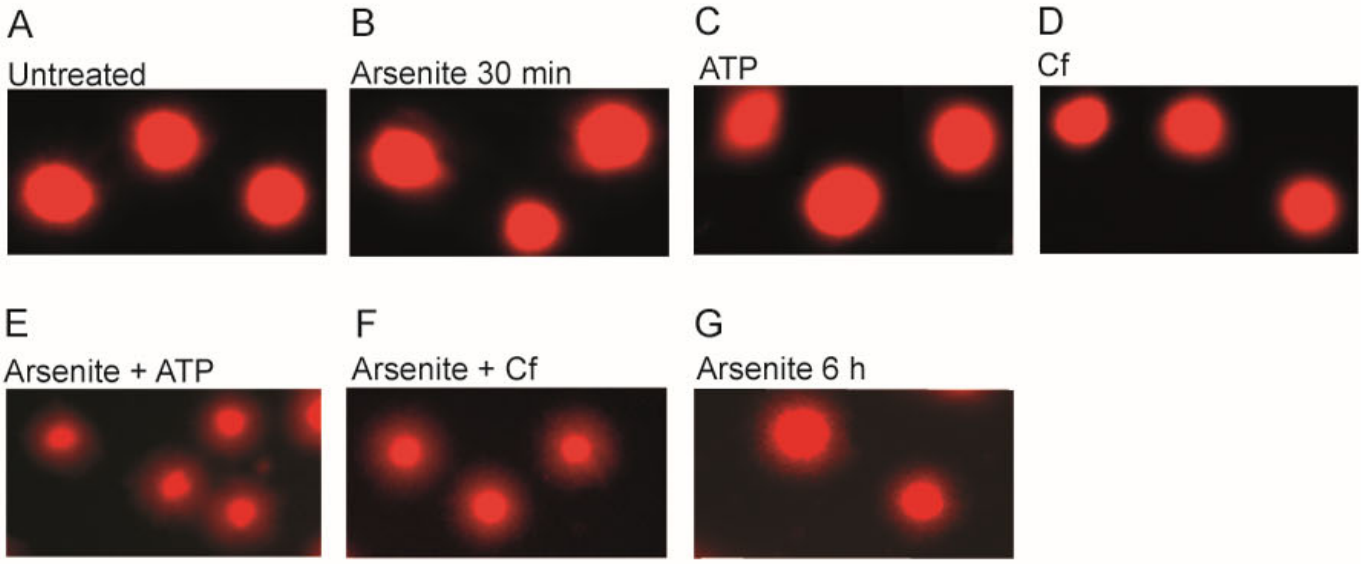

Supplemental Figure 4